FEBS Letters 580 (2006) 4057–4064

Disturbance of cerebellar synaptic maturation in mutant mice lacking BSRPs, a novel brain-specific receptor-like protein family

Taisuke Miyazaki[a,1], Kouichi Hashimoto[b,1], Atsushi Uda[c,d], Hiroyuki Sakagami[e], Yoshitaka Nakamura[c], Shin-ya Saito[c], Miyuki Nishi[c,f], Hideaki Kume[c], Akira Tohgo[c], Izumi Kaneko[c], Hisatake Kondo[e], Kohji Fukunaga[d], Masanobu Kano[b], Masahiko Watanabe[a], Hiroshi Takeshima[c,f,*]

[a] *Department of Anatomy, Hokkaido University, School of Medicine, Sapporo, Japan*
[b] *Department of Cellular Neuroscience, Graduate School of Medicine, Osaka University, Osaka, Japan*
[c] *Department of Medical Chemistry, Tohoku University, Graduate School of Medicine, Sendai, Japan*
[d] *Department of Pharmacology, Graduate School of Pharmaceutical Sciences, Tohoku University, Sendai, Japan*
[e] *Department of Cell Biology, Tohoku University, Graduate School of Medicine, Sendai, Japan*
[f] *Department of Biological Chemistry, Graduate School of Pharmaceutical Sciences, Kyoto University, Kyoto 606-8501, Japan*

Received 9 May 2006; revised 12 June 2006; accepted 15 June 2006

Available online 27 June 2006

Edited by Takashi Gojobori

Abstract **By DNA cloning, we have identified the BSRP (brain-specific receptor-like proteins) family of three members in mammalian genomes. BSRPs were predominantly expressed in the soma and dendrites of neurons and localized in the endoplasmic reticulum (ER). Expression levels of BSRPs seemed to fluctuate greatly during postnatal cerebellar maturation. Triple-knockout mice lacking BSRP members exhibited motor discoordination, and Purkinje cells (PCs) were often innervated by multiple climbing fibers with different neuronal origins in the mutant cerebellum. Moreover, the phosphorylation levels of protein kinase Cα (PKCα) were significantly downregulated in the mutant cerebellum. Because cerebellar maturation and plasticity require metabotropic glutamate receptor signaling and resulting PKC activation, BSRPs are likely involved in ER functions supporting PKCα activation in PCs.**

Keywords: Cerebellum; Endoplasmic reticulum; Knockout mouse; Protein kinase C

1. Introduction

The form and circuitry of the central nervous system develop by a complex process that requires various intracellular signaling systems, as well as the integration of direct and functional interactions between multiple neural and glial cells. Since much remains unknown about the neural developmental processes, it is essential to characterize intracellular and intercellular signaling molecules. Most integral membrane proteins and secretory protein precursors share a signal peptide at their amino terminus. We employed the signal sequence trap method [1], which allowed us to effectively isolate signaling proteins with a wide variety of functions. This report describes the identification of a novel brain-specific transmembrane protein family consisting of three BSRP members, and demonstrates their essential roles in cerebellar synaptogenesis using knockout mice lacking the family members.

2. Materials and methods

2.1. DNA cloning and in situ hybridization

In the survey of membrane proteins from the mouse brain using the signal sequence trap method [1], we isolated the partial BSRP-A cDNA fragment containing the 5′-noncoding sequence and protein-coding sequence for the amino-terminal 128 amino acid residues. Database searches using the cDNA sequence found mouse EST clones that were identical or similar to BSRP-A. To determine the primary structures of BSRP family members, full-length cDNAs were isolated by library screening on the basis of information from the databases. Northern blot analysis in mouse tissues using the cDNAs as probes and in situ hybridization histochemistry using the oligonucleotide probes below were carried out as described previously [2]; the probes are GGTCCTGGGTCCTGCAGACTTGTAGACTTGAGGTCAGATGGAAAC for BSRP-A, TCTGAGGAGGTCCCGACAGGTCATGTCTGTCTGTCTGTCTGTCTG for BSRP-B and GGTCTTAGACATGACCTCTGGAACCCAAGGTCTGTCCATGTCTCC for BSRP-C. The specificities of the probes were checked using brain sections from TKO mice in which the hybridization signals were completely diminished. Total RNA samples were prepared from adult C57BL/6J mouse tissues, and Northern blot analysis was carried out as described previously [3].

2.2. Membrane preparation and immunoblot analysis

Biochemical fractionation of brain microsomal proteins was performed as described previously [4]. The cerebellar homogenate (Ho) was centrifuged at $1000 \times g$ to remove nuclei and large debris (P1). The supernatant fluid (S1) was centrifuged at $10000 \times g$ to obtain the crude synaptosomal fraction (P2), lysed hypo-osmotically and

*Corresponding author. Fax: +81 75 753 4605.
E-mail address: takeshim@pharm.kyoto-u.ac.jp (H. Takeshima).

[1] These authors contributed equally to this work.

Abbreviations: CaMKII, Ca^{2+}/calmodulin-dependent protein kinase II; CF, climbing fiber; EPSC, excitatory postsynaptic current; ER, endoplasmic reticulum; ERK, extracellular signal-regulated kinase; IP3R1, inositol 1,4,5-trisphosphate receptor type 1; mGluR1, metabotropic glutamate receptor subtype 1; PC, Purkinje cell; PF, parallel fiber; PKA, cAMP-dependent protein kinase; PKC, protein kinase C; TKO mice, triple-knockout mice lacking BSRP members; VGluT, vesicular glutamate transporter

doi:10.1016/j.febslet.2006.06.043

centrifuged at 25000 × *g* to pellet the synaptosomal membrane fraction (LP1). The supernatant fluid (LS1) was centrifuged at 165000 × *g* to obtain the synaptic-vesicle-enriched fraction (LP2). Concurrently, the supernatant fluid (S2) above the crude synaptosomal fraction (P2) was centrifuged at 165000 × *g* to obtain the cytosolic fraction (S3) and the light membrane/microsome-enriched fraction (P3). The preparations were subjected to immunoblot analysis, and immunoreactivities were visualized using the ECL chemiluminescence detection system (Amersham). To produce antibodies to BSRP subtypes, rabbits were immunized with keyhole limpet hemocyanin-conjugated with synthetic peptides corresponding to the amino acid residues 61–75 for BSRP-A, residues 73–87 for BSRP-B and residues 69–83 for BSRP-C. To examine phosphoprotein levels, the cerebellum was homogenized in a buffer containing phosphatase inhibitors and the resulting total cerebellar proteins were subjected to immunoblot analysis as described previously [5].

2.3. Knockout mice and behavioral analysis

Knockout mice were created as described previously [6]. The resulting mice carrying targeted mutations in the BSRP-A, B and C genes were crossed with each other, and triple-knockout (TKO) mice lacking all of the members (129 strain and C57BL genetic background) were obtained. The synthetic primers used for genotyping the knockout mice are primer A3 (CGTGGGCTTGACACCTTTCTCAGC), primer A4 (CCCCAGTGAAATACTCCCCTGATCC), primer B2 (CCGTGGTGATGATGGTGGTAGTGAC), primer B3 (CGTCCCTGAAGCAACTCAACTCGG), primer Neo5′a (GCCACACGCGTCACCTTAATATGCG), primer C5 (GAGTGAGCAGAATCCATCAAGAGG), primer C4 (CATCTTCACAGGTGATGCTGTGTC) and primer PneoS (CGCTATCAGGACATAGCGTTGGCTACC). To survey abnormal cerebellar functions of the mutant mice generated, the fixed-bar and rota-rod tests were carried out as described previously [7,8].

2.4. Morphological analysis

Preparation of brain sections, immunofluorescence analysis and immunoelectronmicroscopic observation were carried out as described previously [9]. To examine multiple innervation between climbing fibers (CFs) and Purkinje cells (PCs), triple-fluorescence staining of cerebellar sections was carried out as described previously [8]. Briefly, CFs were anterogradely labeled by injecting dextran Texas red into anesthetized mice at the inferior olive, the mice were fixed after 4 days by transcardial perfusion, and microslicer sections were immunofluorescence-stained with antibodies to calbindin and vesicular glutamate transporter 2 (VGluT2) for confocal microscopic examination.

2.5. Electrophysiological measurements

Sagittal cerebellar slices from mice were prepared and whole-cell recording was made from PCs as described previously [10]. The composition of intracellular solution was as follows (in mM): 60 CsCl, 10 Cs D-gluconate, 20 TEA-Cl, 20 BAPTA, 4 $MgCl_2$, 4 ATP, 0.4 GTP and 30 HEPES (pH 7.3). The composition of the standard bathing solution was as follows (in mM): 125 NaCl, 2.5 KCl, 2 $CaCl_2$, 1 $MgSO_4$, 1.25 NaH_2PO_4, 26 $NaHCO_3$ and 20 glucose, which was bubbled continuously with a mixture of 95% O_2 and 5% CO_2. Bicuculline (10 μM) was always present in the saline to block spontaneous inhibitory postsynaptic currents. Ionic currents were recorded with a patch-clamp amplifier (Axopatch-1D, Axon Instruments). Stimulation and on-line data acquisition were performed using the PULSE software (HEKA, Germany) on a Macintosh computer.

3. Results

3.1. Identification of BSRP family

In our attempt to identify novel transmembrane proteins in the brain, we obtained the partial cDNA for BSRP-A from a mouse library. Cloning the full-length cDNA defined the primary structure of BSRP-A (Fig. S1A). Database searches identified several EST clones encoding proteins similar to BSRP-A, and this information was used to isolate two additional family members, BSRP-B and -C, by cDNA cloning. Therefore, our cloning resulted in the identification of novel transmembrane protein family members in the mouse genome. The overall amino-acid sequence identity is 31% among the family members, and a high homology is detected in several motif sequences. BSRP-C is identical to SEZ-6, whose mRNA is upregulated in response to seizure-inducing reagents in neurons [11]. Putative protein-coding sequences for BSRP family members can be identified from several animal species in the databases, and the human genome carries predicted genes for three BSRP subtypes.

BSRPs share common structural characteristic features as shown in Fig. 1A. Their primary structures carry a signal sequence, a large luminal/extracellular region, a membrane-spanning segment and a short intracellular region. The proposed luminal/extracellular regions contain repeated SCR (short con-

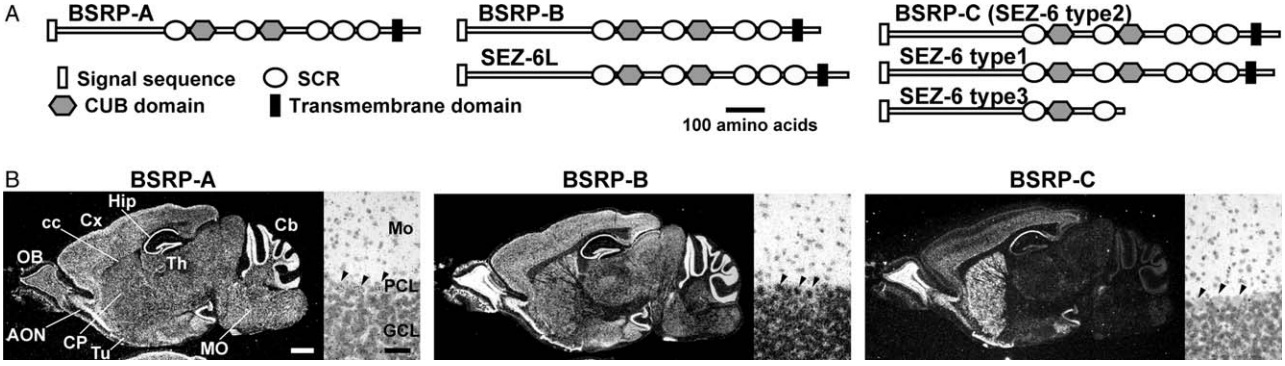

Fig. 1. Structures and distribution of BSRPs. Structural features of BSRP family members (A). Database searches indicated that splicing variants are generated from the BSRP genes, and the most abundant products proposed by our cDNA cloning are shown in the sequence alignment (Fig. S1). The signal sequence, motif sequences for putative intermolecular interaction (CUB and SCR domains) and transmembrane segment are schematically shown. In situ hybridization analysis of BSRP mRNAs in brain (B); dark-field photographs of sagittal sections from adult mouse brain (left panel), and bright-field photographs of the cerebellar cortex (right panel). Note overlapping but distinct spatial expressions of BSRP mRNAs in the adult mouse brain. AON, anterior olfactory nuclei; Cb, cerebellar cortex; cc, corpus callosum; CP, caudate putamen; Cx, cerebral cortex; GCL, granule cell layer; Hip, hippocampal formation; MO, medulla oblongata; Mo, molecular layer; OB, olfactory bulb; PCL, Purkinje cell layer; Th, thalamus; Tu, olfactory tubercle. Arrowheads indicate PCs. Scale bars: 1 mm in left panel and 100 μm in right panel. Signal specificity was confirmed with brain sections from TKO mice in which hybridization signals described above were completely diminished (data not shown). Young adult mice were used for the analysis.

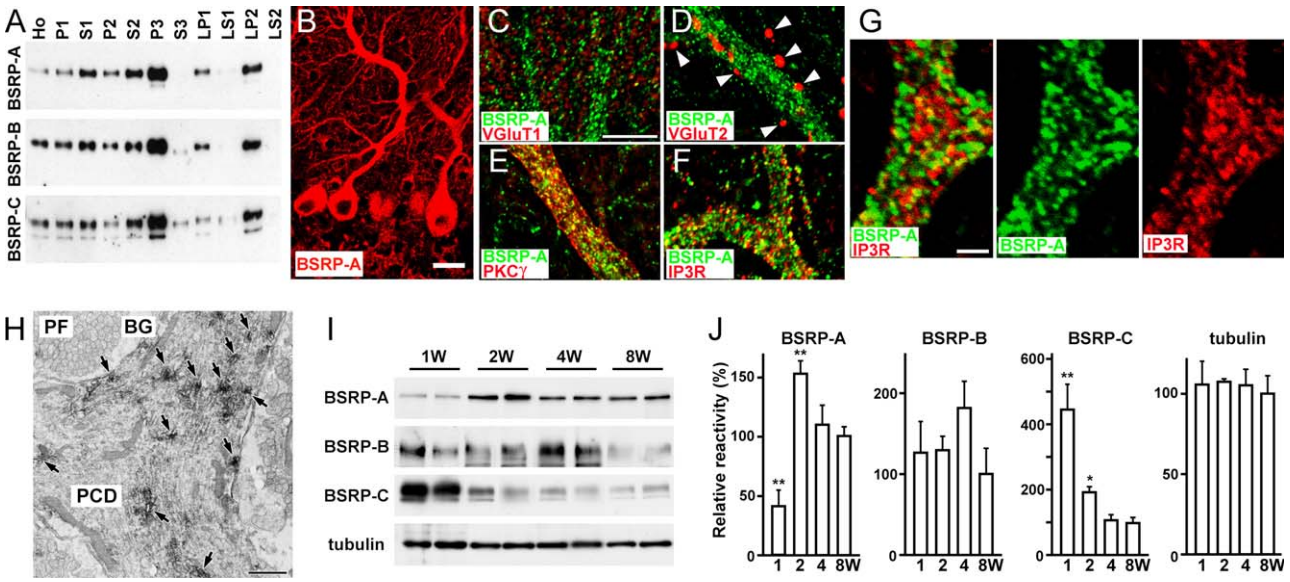

Fig. 2. Expression of BSRPs in cerebellum. Western blot analysis of BSRPs in membrane preparations from cerebellum (A). Fractionated samples (5 μg protein/lane) were analyzed with antibodies specific to BSRP family members. Membrane fractionation and the preparations are described in Section 2, and the molecular sizes of immunoreactive bands are shown in Fig. S2. Immunofluorescence images of BSRP-A in cerebellum (B–G). Among cerebellar cell types, PCs showed the strongest signals for BSRP-A immunoreactivity. Positive signals underneath the PC layer are derived from granular cells, and immunoreactive small cells in the molecular layer are assigned as interneurons supplying inhibitory inputs to PCs (B). In the somatodendritic regions of PCs, BSRP-A-positive signals clearly form puncture structures (C–F). There was no obvious correlation of BSRP-A signals with VGluT1 (marker for PF terminals) or VGluT2 (marker for CF terminals indicated by arrowheads) signals (C, D). BSRP-A signals were detected inside cell-surface PKCγ signals (E), and partially overlap with IP3R1 signals (F, G). Immunoelectronmicroscopic images of BSRP-A in PCs (H). The immunoperoxidase-labeled image demonstrated that BSRP-A is predominantly localized to intracellular membranous organelles likely assigned to sER. Immunogold-labeling analysis confirmed this observation (data not shown). Arrows indicate immunostaining signals. BG, Bergmann glia; PCD, Purkinje cell dendrite; PF, parallel fiber. Scale bars: 10 μm in B, 5 μm in C–F, 2 μm in G, and 1 μm in H. Young adult mice were used for the immunoanatomical analyses. Expression levels of BSRPs during cerebellar maturation in postnatal stages (I, J). Total cerebellar homogenates were prepared from 1–8-week-old mice and analyzed (5 μg/lane) in Western blotting using antibodies to BSRP members (I). The immunoreactivities were digitalized and statistically analyzed (J). The data from 3–5 mice were normalized with the mean values from 8-week-old mice, and indicated by mean ± S.E.M. Significant differences compared with expression in 8-week-old mice are denoted by asterisks ($^{*}P < 0.05$ and $^{**}P < 0.01$ in t test).

sensus repeat for complement C3b/C4b-binding site) and CUB (complement C1r/s-like repeat) domains. Both SCR and CUB domains are often observed in extracellular proteins for the immune system, and are thought to have roles in protein–protein interaction [12,13]. In the intracellular region, BSRPs share a consensus NPXY motif, and potential tyrosine phosphorylation sites were identified by computer searches. The NPXY motif can interact with clathrin, AP-2 and Dab2 in the adaptor protein complex for transmembrane protein sorting [14], and likely restricts the somatodendritic distribution of BSRPs in neurons as described below. Our database searches also revealed the presence of two BSRP-B variants and three BSRP-C variants generated by alternative splicing. BSRP-C variants contain a putative soluble form lacking the transmembrane segment, although it is assigned as a minor product based on its cloning efficiency (data not shown).

3.2. Brain-specific expression and subcellular localization of BSRPs

Expression of BSRPs was shown to be exclusively in the brain by northern blot analysis (Fig. S1B). In situ hybridization histochemistry (Fig. 1B) demonstrated wide expression of BSRP-A and B in the gray matter of the brain with high levels in the olfactory bulb, anterior olfactory nuclei, hippocampal formation and cerebellar cortex. BSRP-A and -B mRNAs were also detected diffusely and weakly in the white matter, such as the corpus callosum and cerebellar medulla. In contrast, expression of BSRP-C mRNA was restricted to the gray matter with higher levels in the forebrain including the olfactory bulb, anterior olfactory nuclei, olfactory tubercle, striatum, hippocampal CA1 pyramidal cell layer and cerebral cortex. Considering that the major cellular constituent in white matter is glial cells, as well as concentrated neuronal distribution in gray matter, the results suggest that BSRP mRNAs are predominantly expressed in neurons. In the cerebellar cortex, both BSRP-A and -B mRNAs were intensely expressed in PCs and granule cells. Positive signals for both mRNAs were also detected in interneurons in the molecular layer. In contrast, BSRP-C mRNA was expressed only faintly in the granule cells.

To examine the subcellular distribution of BSRPs, fractionated cerebellar membrane samples were examined with subtype-specific antibodies (Fig. 2A). In standard cell fractionation (Ho ~ S3), BSRP family members were predominantly recovered in P3 (total microsome). Both antibodies to BSRP-B and -C detected weak immunoreactivity in S3 (soluble fraction including cytosolic and extracellular proteins), suggesting that the proposed soluble minor products are generated by alternative splicing and are localized in extracellular space. By the further fractionation of the membrane preparation (LP1 ~ LS2), BSRP members were found predominantly in LP2 (synaptic and intracellular vesicle fraction) and also weakly detected in LP1 (plasma membrane fraction).

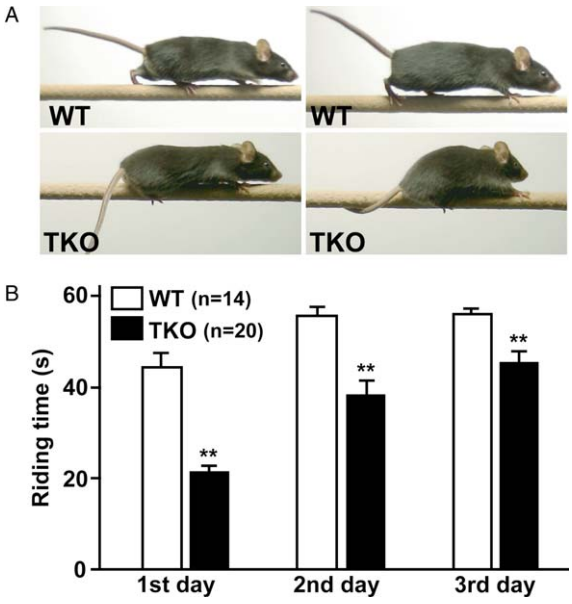

Fig. 3. Motor discoordination in BSRP-TKO mice. Fixed bar test (A). A mouse was placed on a narrow fixed bar, and its behavior was captured. Wild-type mice walked normally on the bar, while TKO mice characteristically showed grasping and pulling with their forepaws and dragging of their hindlimbs. Rota-rod test (B). The time an animal remained on a rotating rota-rod (16 rpm) was measured during training by four trials per day. A maximum of 60 s was allowed for each animal per trial. The data represent mean ± S.E.M., and significant differences compared with controls are denoted by asterisks ($^{**}P < 0.01$ in t test). In the tests, 8–9-week-old mice were examined.

Among the antibodies produced, antibody to BSRP-A could produce specific immunohistochemical signals, as judged by the blank staining in the brain from the knockout mice. In the cerebellar cortex, perikarya and dendrites of PCs, granule cells and molecular layer interneurons were immunopositive with the highest level in PCs (Fig. 2B). At a high magnification, immunofluorescent signals were punctate and densely packed in the perikarya and thick proximal dendrites of PCs (Fig. 2C–F). BSRP-A was not detected in parallel fiber (PF) terminals immunolabeled for VGluT1 or CF terminals immunolabeled for VGluT2, demonstrating its preferential somatodendritic localization. When examined for protein kinase Cγ (PKCγ), which predominantly translocates to the plasmalemma depending on the signaling state, BSRP-A-positive puncta were detected inside plasmalemmal PKCγ signals. BSRP-A-positive puncta in thick dendrites appeared similar in shape and size to inositol 1,4,5-trisphosphate receptor type 1 (IP3R1)-positive sER. The BSRP-A and IP3R1-immunolabeled puncta partially overlapped but were often positioned side by side (Fig. 2G). Immunoelectron microscopy revealed immunoperoxidase reaction products concentrated around tubular or round profiles of membranous organelles (Fig. 2H), and post-embedding immunogold staining confirmed the observation (data not shown). These results, together with the structural and biochemical features, indicate that BSRPs are predominantly localized to the sER.

Next, we examined BSRP expression levels during postnatal cerebellar maturation in mice (Fig. 2I and J). In Western blotting analysis using total cerebellar extracts, BSRP-A expression was remarkably upregulated at 2 weeks after birth, while BSRP-C expression was highest at 1 week and significantly downregulated thereafter. BSRP-B levels showed considerable individual variability but seemed to be relatively constant during the postnatal stages. Developmental maturation of the CF–PC synapse from multiple- to mono-innervation is completed within several postnatal weeks. Therefore, it may be that BSRP family members are involved in cerebellar development and maturation.

3.3. Motor discoordination of knockout mice lacking BSRPs

To examine physiological functions of BSRPs, we generated knockout mice (Fig. S2). The homologous primary structures and overlapping regional distribution suggest functional redundancy among BSRP family members in the brain. Indeed, knockout mice lacking either of the members did not

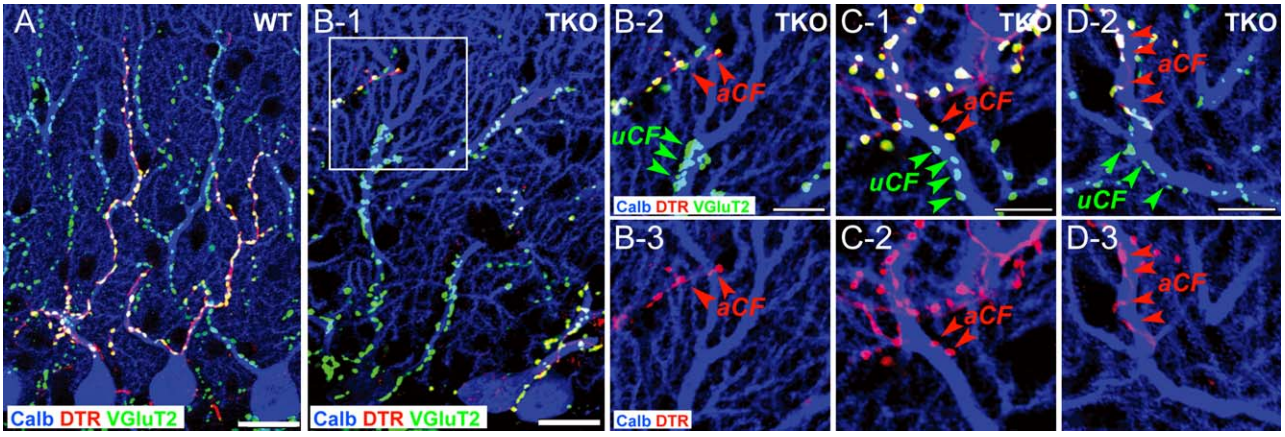

Fig. 4. Multiple CF innervation in BSRP-TKO mice. Triple-fluorescence labeling for calbindin as a marker for PCs (blue), anterogradely dextran Texas red (DTR)-labeling of CFs in part (red) and VGluT2 as a marker for CF terminals (green). In control PCs associated with anterogradely labeled CFs, VGluT2 signals were always covered with DTR signals to yield yellow signals, demonstrating mono-innervation (A). Control PC dendrites were associated with VGluT2-positive CF terminals at regular intervals up to the border between shaft dendrites and spiny branchlets. However, mutant PC dendrites occasionally showed interruption of the VGluT2-fluorescent arrays (boxed region in B-1). High-powered merge and separated micrographs of the boxed region (B-2,3) detected two types of CF terminals derived from different neural origins, DTR-labeled CF (aCF) and unlabeled CF (uCF), on shaft dendrites from a single PC. Similar multiple CF innervation was often detected in TKO mice (C, D). Scale bars: 20 μm in A and B-1, 5 μm in B-2 to D-3. In the analysis, 9–12-week-old mice were examined.

show clear abnormalities. Because the genes for BSRP family members are localized on different mouse chromosomes, we produced triple-knockout mice lacking all of BSRPs (TKO mice) by interbreeding the single knockout mice. Resulting TKO mice were still healthy under our conventional housing conditions, and showed no obvious defects in development and reproduction.

TKO mice exhibited an abnormal behavior when placed on a narrow bar (fixed-bar test). Wild-type mice walked quickly and proficiently, whereas TKO mice walked slowly and were essentially crawling on the bar (Fig. 3A). Moreover, TKO mice frequently stopped and wound their tails around the bar. In the rota-rod test (Fig. 3B), TKO mice failed to stay on a rotating rod in comparison with wild-type mice, and showed significant impairments in all the trials. Although TKO mice could improve rota-rod performance during the training, the degree of improvement was relatively poor. Therefore, TKO mice bear impaired motor coordination. In the rota-rod task, single-knockout mice lacking BSRP-B exhibited a mild impairment, while double-knockout mice lacking both BSRP-A and C retained a normal performance similar to that of wild-type mice (data not shown). These observations likely suggest that BSRP family members are functionally redundant in cerebellar functions.

3.4. Multiple CF–PC innervation in BSRP-TKO mice

TKO mice exhibited no abnormalities in basic cerebellar histology and cytology. No abnormalities in cerebellar size, trilaminar organization in the cerebellar cortex, distributions of inhibitory terminals, somata and dendritic shafts of PCs and of PF terminals on dendritic spines were detected in the TKO cerebellum (Fig. S3A-F). Moreover, TKO mice retained normal PF–PC synapses in structure, distribution and density (Fig. S3G-I).

Phenotypic abnormalities of TKO mice were seen in dendritic innervation by CFs. In TKO mice, VGluT2 signals (marker for CF terminals) mainly appeared at regular intervals and were distributed within a defined territory on PC dendrites. However, shaft dendrites of PCs often had segments associated with no CF terminals in the mutant cerebellum, suggesting abnormal CF-PC innervation. We next confirmed the observation by triple-fluorescence labeling for CFs and PCs. Cerebellar sections were prepared from mice injected with an anterograde trace of dextran Texas red into the inferior olive for partially fluorescence-labeling CFs, and were immunofluorescence-stained with antibodies against calbindin (blue) and VGluT2 (green) for confocal-microscopic analysis. In wild-type mice, the signals of anterogradely labeled CFs (aCFs) were observed precisely according to the branching of shaft dendrites (Fig. 4A). Moreover, terminal swellings of the aCFs overlapped completely with VGluT2 and turned to yellow in the merged image, thus representing mono-innervation. In TKO mice, morphological evidence of multiple innervation was demonstrated with blank segments at dendrites (Fig. 4B-1). In the boxed region, a shaft dendrite proximal to the blank segment was innervated by anterogradely unlabeled CF (uCF, green or blue), whereas its distal portion was innervated by aCF (yellow or white puncta) that leaped from the neighbor (Fig. 4B-2,3). Multiple innervation in TKO mice was also addressed in shaft dendrites that were innervated regularly and continuously by VGluT2-positive CF terminals (Fig. 4C and D); a portion of shaft dendrites was innervated by aCF, whereas the rest was considered as an uCF-projection area.

3.5. Electrophysiological abnormalities of CF–PC synapse in BSRP-TKO mice

To further analyze CF–PC synapses in TKO mice, we conducted whole-cell patch clamp recording in cerebellar slices. In the majority of PCs from wild-type mice, a clearly discernible excitatory postsynaptic current (EPSC) was elicited in an all-or-none fashion, indicating that most PCs were innervated by single CFs (Fig. 5A and D). In contrast, the percentage of PCs

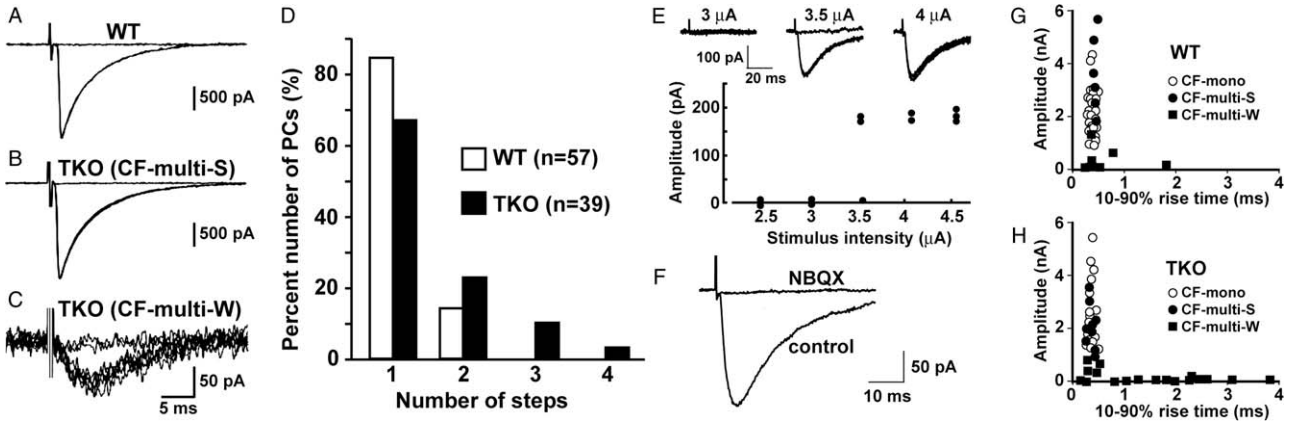

Fig. 5. Electrophysiological abnormalities of CF–PC synapses in BSRP-TKO mice. Sample traces of EPSCs elicited by stimulating CFs in wild-type (A) and BSRP-TKO mice (B, C). CFs were stimulated in the granule cell layer at 0.2 Hz, and two to three traces are superimposed at each threshold stimulus intensity. Holding potential was −20 mV for A and B and −80 mV for C. Responses in B and C were recorded from the same PC. Holding potential was corrected for liquid junction potential. Frequency distribution histogram showing the number of discrete steps of EPSCs (D). All or none behavior of a slow EPSC elicited in a BSRP-TKO PC (E). EPSCs were elicited five times at each stimulus intensity and the peak amplitudes were plotted against the stimulus intensity. At 3.5 μA, one of the five stimuli failed to elicit an EPSC. Holding potential was −80 mV. Slow EPSCs are mediated by AMPA receptors (F). The slow EPSC is completely blocked by bath-applied NBQX (10 μM). The same results were observed in 6 slow EPSCs. Holding potential was −70 mV. The amplitudes of CF-EPSCs (measured at a holding potential of −20 mV) are plotted against the 10–90% rise time for wild-type (G) and BSRP-TKO (H) mice. Open circles, closed triangles and closed circles represent CF-mono, CF-multi-S and CF-multi-W, respectively. Note that the number of CF-multi-W with small amplitude and slow rise time was apparently higher in BSRP-TKO mice than in wild-type mice. In the analysis, at least 3 mice (~5 weeks old) were examined.

with two or more discrete EPSC steps was higher in TKO mice than in wild-type mice (Fig. 5B–D) ($P < 0.05$, χ^2 test). Multiple EPSCs were elicited in 9 of 57 (16%) wild-type PCs and 14 of 39 (36%) TKO PCs. However, no perceptible abnormalities were detected in the basic properties of EPSCs elicited by stimulating mono-innervating CFs (Fig. S4, Tables S1 and S2).

In TKO mice, PCs with multiple EPSC steps often had EPSCs with small amplitudes and slow rise times (Fig. 5C). These EPSCs were elicited in an all-or-none fashion (Fig. 5E) and showed clear paired-pulse depression (data not shown), indicating that they were elicited by stimulating CFs. These slow EPSCs were markedly enhanced by DL-threo-β-benzyloxyaspartate (100 μM), a blocker of glutamate transporter (data not shown), and were completely blocked by an AMPA receptor antagonist, NBQX (10 μM) (Fig. 5F). These results indicate that the slow EPSCs do not involve glutamate transporter currents but are mediated by AMPA receptors. To examine CF innervation in more detail, we classified CFs into three groups as described previously [10] and plotted the peak amplitudes against the 10–90% rise times of CF-EPSCs elicited by stimulating respective CFs (Fig. 5G and H). In an individual multiply-innervated PC, the CF that elicited the largest CF-EPSC was termed "CF-multi-S (Strong)" and the remaining of CFs were termed "CF-multi-W (Weak)" (because they were inevitably weaker than 'CF-multi-S'). The CF of mono-innervated PC was termed "CF-mono". CF-mono and CF-multi-S showed similar distributions both in wild-type (Fig. 5G) and TKO (Fig. 5H). The 10–90% rise times for CF-mono/CF-multi-S were all shorter than 1 ms and the amplitudes were in the range of 1–6 nA at a holding potential of −20 mV. In contrast, the number of CF-multi-W with rise times slower than 1 ms was apparently higher in TKO mice than in wild-type mice. All of these responses had small amplitudes less than 70 pA at a holding potential −20 mV (Fig. 5H). Therefore, the abnormal PCs in TKO mice tend to be innervated by one strong CF with a fast EPSC rise time plus a few weak CFs with slower rise times. Because ectopic CFs innervating distal dendrites elicit EPSCs with slow rise times in GluRδ2 knockout mice [15], these results suggest the existence of weak and ectopic CF innervation of PC dendrites in TKO mice. This notion is consistent with the immunohistochemical data demonstrating ectopic CF–PC innervation on PC dendrites in TKO mice (Fig. 4).

3.6. Reduced autophosphorylation of PKCα in BSRP-TKO cerebellum

Recent studies have demonstrated that synaptic maturation and plasticity require vital functions of various protein kinases. To examine whether abnormal kinase activities are associated with the TKO cerebellum, Western blot analysis was carried out using antibodies to phosphopeptides. Our analysis detected normal PKCα contents but reduced phospho-PKCα levels in the TKO cerebellum (Fig. 6). Because the PKCα autophosphorylation correlates well with its kinase activity and is abundantly expressed in PCs among cerebellar cell types [16,17], the observations likely suggest impaired PKCα activity under basal conditions in TKO PCs. However, no significant differences were suggested in PKCγ, Ca^{2+}/calmodulin-dependent protein kinase II (CaMKII), extracellular signal-regulated kinase (ERK) and cAMP-dependent protein kinase (PKA) activities between wild-type and TKO mice. Western blotting also detected normal density and distribution of major synaptic components of PCs in the TKO cerebellum (Fig. S5).

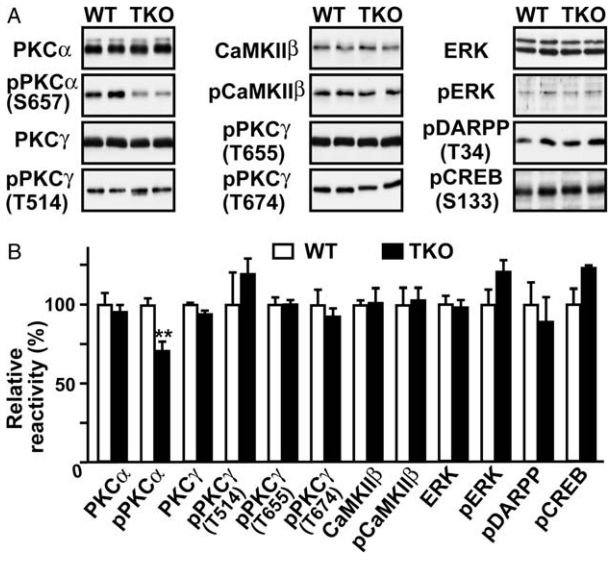

Fig. 6. Reduced phospho-PKCα in BSRP-TKO cerebellum. Total cerebellar proteins were analyzed (10 μg/lane) by Western blotting using antibodies to phospho-PKCα at S657, phospho-PKCγ at T514, T655 and T674, phospho-CaMKIIβ, phospho-ERK, phospho-DARPP32 at T34 and phospho-CREB at S133. Their total protein levels were also determined with antibodies recognizing both phosphorylated and non-phosphorylated forms. Representative immunoreactivity (A) and summarized immunoreactivity normalized with the values of wild-type mice (B) are shown. DARPP32 and CREB are known as PKA target proteins. The data represent mean ± S.E.M. from at least 4 mice (10–13 weeks old), and a significant difference compared with control is marked by asterisks (** $P < 0.01$ in t test).

4. Discussion

The results present here demonstrate that CF–PC synaptic maturation is impaired in TKO mice. During developmental maturation from the multiple- to mono-innervation, major roles of BSRPs may be assigned to the PC side rather than the CF terminal, because of their somatodendritic distribution in neurons. The functional importance of mono-CF innervation was recently demonstrated by various mutant animals exhibiting motor discoordination. The causes of multiple innervation in the animal models so far reported can be categorized into three distinct mechanisms. First, irregular PF–PC synapses induce multiple innervation, based on the results of hypogranular animals including X-ray-irradiated rats [18] and knockout mice lacking GluR δ2 subunit [19]. TKO mice retaining normal density of granular cells and regular PF–PC synaptogenesis (Fig. S3) are not assigned to this category. Second, Ca^{2+} entry through the P/Q-type voltage-gated Ca^{2+} channel in PCs is essential for the establishment of mono-innervation. Knockout mice lacking the P/Q-type channel manifest a diminished territory of CF innervation and proximal expansion of PF innervation down to the PC soma [20]. Because CF and PF innervations with normal territories were observed in TKO mice (Fig. S3), it is unlikely that BSRPs are functionally associated with the P/Q-type channel. Third, metabotropic glutamate receptor subtype 1 (mGluR1)-mediated signaling in PCs is essential for mono-innervation, based

on the phenotypes in knockout mice lacking mGluR1, Gαq of the trimeric GTP-binding protein, phospholipase Cβ4 and PKC [21–24]. This signal cascade also produces IP3 triggering IP3R1-mediated Ca^{2+} release. Although TKO mice showed atypical multiple CF-innervation producing irregular EPSCs with the slow time course and small amplitude (Fig. 5), such abnormal electrophysiological features have not been reported in mutant mice lacking the mGluR1 cascade. However, mutant mice lacking the mGluR1 cascade and our TKO mice share several histological abnormalities, including multiple CF-innervation observed within the normal territory of PC dendrites. Moreover, BSRPs as residents on the endoplasmic reticulum (ER) are partially co-localized with IP3R1 in PCs (Fig. 2), and PKCα hypoactivity is proposed in TKO PCs under basal conditions (Fig. 6). Recent studies indicate that both PKCα and PKCγ contribute to functional maturation of PCs and cerebellar plasticity [16,17,25,26]. Therefore, it is possible that BSRPs in the ER participate in the mGluR1 signaling, and that CF–PC synaptic maturation is disturbed by impaired PKCα activity in TKO PCs.

Activation of classical PKC subtypes, including PKCα and PKCγ, requires both Ca^{2+} and diacylglycerol-induced translocation from the cytosol to membranous sites [16]. It may seem puzzling that the TKO cerebellum retained normal PKCγ activity yet bear impaired PKCα activity. In cultured cells, PKC subtypes predominantly translocate to the cell membrane upon their activation, but the attachment of PKCα with the ER membrane has also been reported [27,28]. The distinct subcellular distribution between PKC subtypes may be the direct cause of the PKCα-specific hypoactivity in the TKO cerebellum. Because BSRPs are localized on the sER as intracellular Ca^{2+} stores, it can be hypothesized that BSRPs would be involved in Ca^{2+}-handling of the ER through the predicted intermolecular interaction using the luminal SCR and CUB domains. For example, the loss of BSRPs might induce insufficient ER Ca^{2+} release to prevent the full activation of PKCα localized on the ER during the mGluR1 signaling in PCs. Because database searches found no BSRP homologue in non-neuronal tissues, BSRPs likely contribute to specialized ER functions in neurons. In order to elucidate the bona fide molecular roles of BSRP members, we need to further examine abnormalities in several neural sites in TKO mice as a useful model system.

Acknowledgements: We thank Miyuki Kameyama for technical assistance in mutant mouse generation, Hidemi Shimizu for production of anti-GFAP antibody, and Motokazu Uchigashima for immunoblot analysis. This work was supported in part by grants from the Ministry of Education, Culture, Sports, Science and Technology of Japan, the Ministry of Health and Welfare of Japan, and the Mitsubishi Foundation.

Appendix A. Supplementary data

Supplementary data associated with this article (Figs. S1–S5 and Tables SI and SII) can be found, in the online version, at doi:10.1016/j.febslet.2006.06.043.

References

[1] Tashiro, K., Tada, H., Heiker, R., Shirozu, M., Nakano, T. and Honjo, T. (1993) Signal sequence trap: a cloning strategy for secreted proteins and type I membrane proteins. Science 261, 600–603.
[2] Nishi, M., Sakagami, H., Komazaki, S., Kondo, H. and Takeshima, H. (2003) Coexpression of junctophilin type 3 and type 4 in brain. Mol. Brain Res. 118, 102–110.
[3] Takeshima, H., Komazaki, S., Nishi, M., Iino, M. and Kangawa, K. (2000) Junctophilins: a novel family of junctional membrane complex proteins. Mol. Cell 6, 11–22.
[4] Nakamura, M., Sato, K., Fukaya, M., Araishi, K., Aiba, A., Kano, M. and Watanabe, M. (2004) Signaling complex formation of phospholipase Cβ4 with mGluR1α and IP3R1 at the perisynapse and endoplasmic reticulum in the mouse brain. Eur. J. Neurosci. 20, 2929–2944.
[5] Fukunaga, K., Stoppini, L., Miyamoto, E. and Muller, D. (1993) Long-term potentiation is associated with an increased activity of Ca^{2+}/calmodulin-dependent protein kinase II. J. Biol. Chem. 268, 7863–7867.
[6] Takeshima, H., Iino, M., Takekura, H., Nishi, M., Kuno, J., Minowa, O., Takano, H. and Noda, T. (1994) Excitation-contraction uncoupling and muscular degeneration in mice lacking functional skeletal muscle ryanodine-receptor gene. Nature 369, 556–559.
[7] Nishi, M., Hashimoto, K., Kuriyama, K., Komazaki, S., Kano, M., Shibata, S. and Takeshima, H. (2002) Motor discoordination in mutant mice lacking junctophilin type 3. Biochem. Biophys. Res. Commun. 292, 318–324.
[8] Tohgo, A., Eiraku, M., Miyazaki, T., Miura, E., Kawaguchi, S., Nishi, M., Watanabe, M., Hirano, T., Kengaku, M. and Takeshima, H. (2006) Impaired cerebellar functions in mutant mice lacking DNER. Mol. Cell. Neurosci. 31, 326–333.
[9] Sakai, K., Shimizu, H., Koike, T., Furuya, S. and Watanabe, M. (2003) Neutral amino acid transporter ASCT1 is preferentially expressed in L-Ser-synthetic/storing glial cells in the mouse with transient expression in developing capillaries. J. Neurosci. 23, 550–560.
[10] Hashimoto, K. and Kano, M. (2003) Functional differentiation of multiple climbing fiber inputs during synapse elimination in the developing cerebellum. Neuron 38, 785–796.
[11] Shimizu-Nishikawa, K., Kajiwara, K. and Sugaya, E. (1995) Cloning and characterization of seizure-related gene, SEZ-6. Biochem. Biophys. Res. Commun. 216, 382–389.
[12] Hourcade, D., Holers, V.M. and Atkinson, J.P. (1989) The regulators of complement activation (RCA) gene cluster. Adv. Immunol. 45, 381–416.
[13] Bork, P. and Beckmann, G. (1993) The CUB domain: a widespread module in developmentally regulated proteins. J. Mol. Biol. 231, 539–545.
[14] Bonifacino, J.S. and Traub, L.M. (2003) Signals for sorting of transmembrane proteins to endosomes and lysosomes. Annu. Rev. Biochem. 72, 395–447.
[15] Hashimoto, K., Ichikawa, R., Takechi, H., Inoue, Y., Aiba, A., Sakimura, K., Mishina, M., Hashikawa, T., Konnerth, A., Watanabe, M. and Kano, M. (2001) Roles of glutamate receptor delta 2 subunit (GluRdelta2) and metabotropic glutamate receptor subtype 1 (mGluR1) in climbing fiber synapse elimination during postnatal cerebellar development. J. Neurosci. 21, 9701–9712.
[16] Metzger, F. and Kapfhammer, J.P. (2003) Protein kinase C: its role in activity-dependent Purkinje cell dendritic development and plasticity. Cerebellum 2, 206–214.
[17] Saito, N. and Shirai, Y. (2002) Protein kinase C gamma (PKC gamma): function of neuron specific isotype. J. Biochem. (Tokyo) 132, 683–687.
[18] Altman, J. and Anderson, W.J. (1972) Experimental reorganization of the cerebellar cortex. I. Morphological effects of elimination of all microneurons with prolonged X-irradiation started at birth. J. Comp. Neurol. 146, 355–406.
[19] Ichikawa, R., Miyazaki, T., Kano, M., Hashikawa, T., Tatsumi, H., Sakimura, K., Mishina, M., Inoue, Y. and Watanabe, M. (2002) Distal extension of climbing fiber territory and multiple innervation caused by aberrant wiring to adjacent spiny branchlets in cerebellar Purkinje cells lacking glutamate receptor δ2. J. Neurosci. 22, 8487–8503.
[20] Miyazaki, T., Hashimoto, K., Shin, H.S., Kano, M. and Watanabe, M. (2004) P/Q-type Ca^{2+} channel alpha1A regulates

synaptic competition on developing cerebellar Purkinje cells. J. Neurosci. 24, 1734–1743.
[21] Kano, M., Hashimoto, K., Chen, C., Abeliovich, A., Aiba, A., Kurihara, H., Watanabe, M., Inoue, Y. and Tonegawa, S. (1995) Impaired synapse elimination during cerebellar development in PKCγ mutant mice. Cell 83, 1223–1231.
[22] Kano, M., Hashimoto, K., Kurihara, H., Watanabe, M., Inoue, Y., Aiba, A. and Tonegawa, S. (1997) Persistent multiple climbing fiber innervation of cerebellar Purkinje cells in mice lacking mGluR1. Neuron 18, 71–79.
[23] Kano, M., Hashimoto, K., Watanabe, M., Kurihara, H., Offermanns, S., Jiang, H., Wu, Y., Jun, K., Shin, H.S., Inoue, Y., Simon, M.I. and Wu, D. (1998) Phospholipase Cβ4 is specifically involved in climbing fiber synapse elimination in the developing cerebellum. Proc. Natl. Acad. Sci. USA 95, 15724–15729.
[24] Offermanns, S., Hashimoto, K., Watanabe, M., Sun, W., Kurihara, H., Thompson, R.F., Inoue, Y., Kano, M. and Simon, M.I. (1997) Impaired motor coordination and persistent multiple climbing fiber innervation of cerebellar Purkinje cells in mice lacking Gαq. Proc. Natl. Acad. Sci. USA 94, 14089–14094.
[25] Chung, H.J., Steinberg, J.P., Huganir, R.H. and Linden, D.J. (2003) Requirement of AMPA receptor GluR2 phosphorylation for cerebellar long-term depression. Science 300, 1751–1755.
[26] Leitges, M., Kovac, J., Plomann, M. and Linden, D.J. (2004) A unique PDZ ligand in PKCalpha confers induction of cerebellar long-term synaptic depression. Neuron 44, 585–594.
[27] Goodnight, J.A., Mischak, H., Kolch, W. and Mushinski, J.F. (1995) Immunocytochemical localization of eight protein kinase C isotypes overexpressed in NIH3T3 fibroblasts. J. Biol. Chem. 270, 9991–10001.
[28] Stensman, H., Raghunath, A. and Larsson, C. (2004) Autophosphorylation suppresses whereas kinase inhibition augments the translocation of protein kinase Calpha in response to diacylglycerol. J. Biol. Chem. 279, 40576–40583.